



Probabilistic Risk Assessment of Livestock Snow Disasters in the Qinghai-Tibetan Plateau

Tao Ye^{1,2}, Weihang Liu^{1,3}, Peijun Shi^{1,2}, Yijia Li^{1,2*}, Jidong Wu^{1,2} and Qiang Zhang^{1,2}

¹Key Laboratory of Environmental Change and Natural Disaster, Ministry of Education, State Key Laboratory of Earth Surface Processes and Resource Ecology, Faculty of Geographical Science, Beijing Normal University, Beijing 100875, China;

²Academy of Disaster Reduction and Emergency Management, Ministry of Civil Affairs and Ministry of Education, Beijing 100875, China

³School of Geographic Science, East China Normal University, Shanghai 200241, China

Correspondence to: Yijia Li(liyijia@mail.bnu.edu.cn)

Abstract. Understanding risk using a quantitative risk assessment offers critical information for risk-informed reduction actions, investing in building resilience, and planning for adaptation. This study develops an event-based probabilistic risk assessment model for livestock snow disasters in the Qinghai-Tibetan Plateau (QTP) region and derives risk assessment results based on historical climate conditions (1980–2015) and present-day prevention capacity. In the model a hazard module was developed to identify/simulate individual snow disaster events based on boosted regression trees. Together with a fitted quantitative vulnerability function, and exposure derived from vegetation type and grassland carrying capacity, risk metrics based on livestock mortality and mortality rate were estimated. In our results, high risk regions include the Nyainqêntanglha Range, Tanggula Range, Bayankhar Mountains and the region between the Kailas Range and neighbouring Himalayas. In these regions, annual livestock mortality rates were estimated as $> 2\%$ and mortality was estimated as > 2 sheep unit/km² at a return period of 1/20 a. Prefectures identified with extremely high risk included Yushu in Qinghai Province and Naqu, Shigatse, Linzhi, and Nagri in the Tibet Autonomous Region. In these prefectures, a snow disaster event with return period of 1/20 a or higher can easily claim a total loss of more than 200,000 sheep units. Our event-based PRA results provide a quantitative reference for preparedness and insurance solutions in reducing mortality risk. The methodology developed here can be further adapted to future climate change risk analyses and provide important information for planning climate change adaption in the QTP region.

1 Introduction

Livestock snow disasters are serious winter extreme weather events that widely occur in central-to-east Asian temperate steppe and alpine steppes (Li et al., 2018; Tachiiri et al., 2008). In the pastoral areas of these regions, heavy snow fall leads to thick and long-lasting snow cover, making forage unavailable or inaccessible (Fernández-Giménez et al., 2015). Together with extremely low temperature and strong wind, it severely inhibits natural grazing, claims considerable livestock mortality, and brings devastating impacts to the livelihoods of local herders, even threatening their survival (Wang et al., 2013a). In



response to threats from livestock snow disasters, great efforts have been devoted to understanding their mechanism as a complicated interaction between precipitation, vegetation, livestock, and herding communities (Shang et al., 2012; Sternberg, 2017); the major drivers of (socioeconomic) vulnerability (Fernández-Giménez et al., 2012; Wang et al., 2014; Wei et al., 2017); and key factors that could foster adaptive capacity and community resilience (Fernández-Giménez et al., 2015).

5 Attempts have been made to develop techniques, such as snow disaster monitoring, forecasting, and rapid assessment, to provide critical information for prevention and addressing emergencies (Wang et al., 2013b; Yin et al., 2017).

Disaster risk is a measure of uncertain consequences. The Sendai Framework outlines the importance of risk assessment as a critical means of understanding disaster risk and a prerequisite for other actions, such as risk-based investment for resilience and adaptation (UNISDR, 2015). For livestock snow disasters, researchers have followed the mainstreaming risk assessment

10 methodology by framing risk as the product of hazard, vulnerability, and exposure, $\text{Risk} = \text{Hazard} \times \text{Exposure} \times \text{Vulnerability}$ (Jongman et al., 2015; Kinoshita et al., 2018; Shi and Kaspersen, 2015). However, two very different approaches can be used, which derive quite different risk metrics. The first type employs an ordinal risk assessment framework in which the risk index is derived by integrating several indices representing different components of risk (e.g., the world risk report; Birkmann and Welle, 2016). Several ordinal risk assessment studies have been conducted for Inner

15 Mongolia and the QTP of China (Li et al., 2014; Liu et al., 2014a; Wu et al., 2007). This ordinal approach for risk assessment is flawed in its output: it offers only rankings but no quantitative information of the underlying risk, i.e. the uncertainty of consequences. Consequently, it can be valuable for policy-making but can hardly support risk - informed decisions, e.g. insurance pricing or cost-benefit analysis.

The other risk assessment approach is quantitative, often called the probabilistic risk assessment (PRA), in which risk is

20 measured with a probability distribution of socioeconomic losses (consequences). In the state-of-the-art PRA framework, risk can be estimated by projecting/translating the probability distribution of a hazard via a “dose-response” function (the vulnerability function) (Carleton and Hsiang, 2016). Such a projection/translating can be conducted using analytical methods, or in a more popular sense, carried out via discrete simulation, an approach widely used in catastrophic risk models (Michel-Kerjan et al., 2013). However, studies applying PRA to livestock snow disasters have been limited. Bai et al. (2011)

25 published one of the first trials in applying the PRA framework to a livestock snow disaster risk assessment. In their study, winter season (November to April of the preceding year) average daily snow depth was used to describe snow hazard intensity. Physical vulnerability, a function of livestock mortality rate in response to snow depth, was fitted using historical case data. Using annual average snow depth computed from satellite-retrieved data, return-period livestock mortality and mortality rates were derived as the final risk metrics. Based on their method, quantitative livestock snow disaster risk were

30 mapped nationwide in China (Shi, 2011). The major flaw of this method was the mismatch between the event-based vulnerability function and annual measure of snow hazard. In another work focusing on Mongolia, a vulnerability function trained from a tree-based model was used, but still on an annual basis. They inputted snow water equivalence in climate scenarios to estimate the frequency of anomalous livestock loss rates $>5\%$ or $>17\%$ for 2010–2099 (Tachiiri and Shinoda, 2012). Compared to earlier works, they successfully extended the framework to future climate change analysis, but they did



not report many details describing the final risk metrics. Ye et al. (2017) further extended the PRA framework to support insurance design and pricing. They focused on the risk of economic stress to local herders due to increased feeding expenditures induced by long-lasting thick snow cover in eastern Inner Mongolia but did not analyze livestock mortality issues.

- 5 In this study, we developed an event-based PRA method for present and future livestock snow disaster risk assessments for the QTP region. There are three major aims of this study: 1) Develop a hazard module that can identify/capture snow disaster event based on daily weather data. It is the basis for any event-based modelling attempts, and is particularly important for regions where historical records are absent and for future risk assessment where observations and records are not yet available and variabilities from future climate change will exist. 2) Set up an event-based PRA framework for livestock snow disaster risk assessment by integrating snow disaster event (hazards), livestock vulnerability, and exposure together to derive a probabilistic quantification of risk. 3) Derive the risk metrics for livestock mortality risk in the QTP and offer risk-informed reduction implications.

Worldwide, the QTP suffers from some of the highest livestock snow disasters due to its large area of snow cover area, long-lasting snow cover days, and nomadic grazing. This region is also a hot spot in climate change. Quantitative risk assessments for the present day will likely be a significant source of information for disaster risk reduction. In addition, the framework can be adapted for livestock mortality in snow disasters in the context of future climate change analysis, and therefore support climate adaptation planning for local government and herding communities.

2. Materials and methods

We followed the PRA approach proposed by Carleton and Hsiang (2016), and applied the concept of event-based modelling in catastrophic risk models (Michel-Kerjan et al., 2013). The event-based modelling approach was framed using state-of-the-art three-element risk modelling, hazard, exposure, and vulnerability (Kinoshita et al., 2018; Muis et al., 2015) to model losses claimed by individual events. Then PRA was achieved through repetition of individual event modelling, in which a large number of events were drawn from the full distribution of hazards, given the predicted losses/consequences from individual events, from which a full distribution of disaster loss can be obtained (Fig. 1).

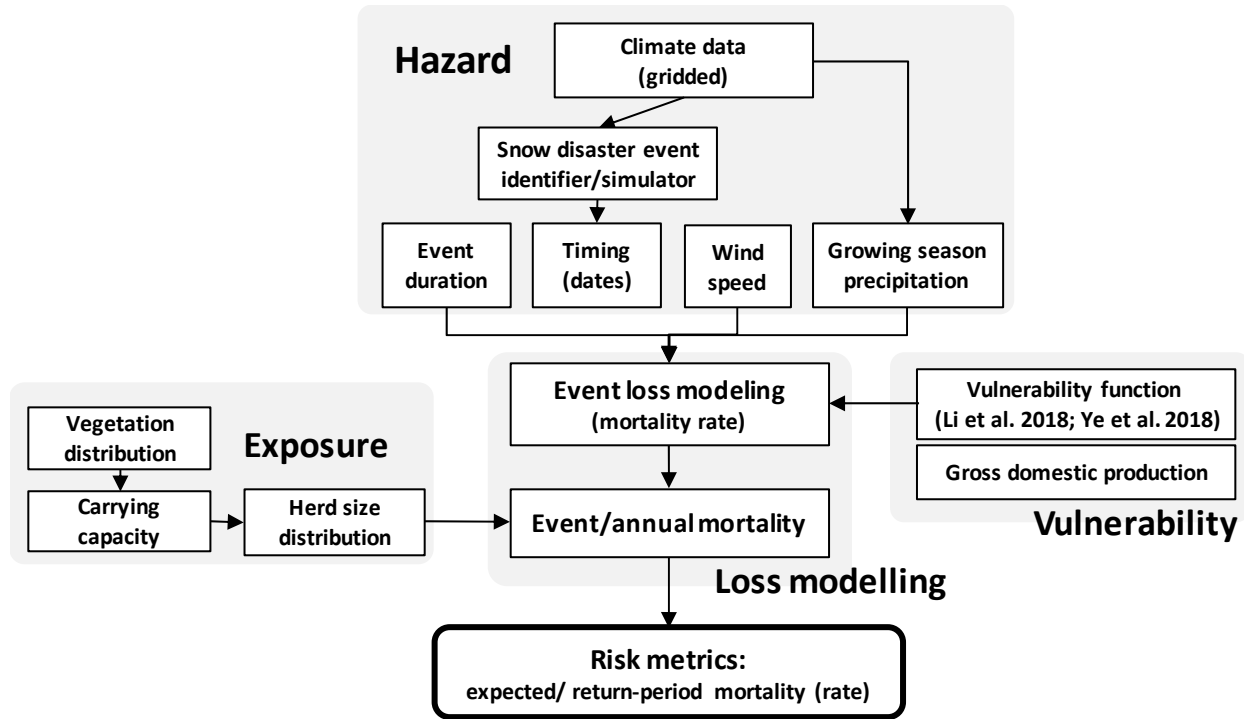


Fig. 1 Probabilistic Risk Assessment Framework for Livestock Snow Disasters in the Qinghai-Tibetan Plateau (QTP) region

2.1 Vulnerability function

Vulnerability is the critical function that links dose (hazard inputs) and response (loss estimates) (Carleton and Hsiang, 2016). For livestock snow disasters, a set of vulnerability functions have been estimated linking livestock mortality (rate) to snow disaster duration, during disaster environmental stress, summer season vegetation productivity, and disaster prevention capacity (Fang et al., 2016; Wang et al., 2016). To fulfil the goal of event-based modelling, the vulnerability relationship must be built on event basis. Therefore, the results from (Li et al., 2018; Ye et al., 2018) were considered. Following their suggestion from the multi-method comparison, we chose the predictive version of the generalized additive model,

$$\ln LR = s(Duration) + s(Wind) + s(P) + s(GDP), \quad (1)$$

where, livestock mortality rate induced by a snow disaster is determined by disaster duration (*Duration*), during disaster maximum daily mean wind speed (*Wind*), growing season (May-Sep) aggregate precipitation (*P*), and prevention capacity as measured by gross domestic production (*GDP*) of the underlying county. The predictive function has a deviance-based R^2 of 0.672, and good predictive power compared to random forest and boosted regression tree models.

Given such a relationship, the vulnerability is a truly dose-response function between livestock mortality rate (mortality/herd size) and snow hazard intensity together with other environmental stressors and prevention capacity, as proposed by



(Carleton and Hsiang, 2016). Different from simply defining vulnerability as the loss rate (Jongman et al., 2015; Kinoshita et al., 2018), the potential influence from socioeconomic development is embedded in the vulnerability function.

2.2 Hazard

Hazard module is critical in our event-based PRA method, and its needs to identify individual snow disaster events, and provide provide the exact timing (starting and ending dates) of each event, based on which *Duration* and *Wind* can be derived. Such information, nevertheless, are not so straightforward to obtain. For the historical period, there are no ready-to-use snow disaster event datasets at the grid level. The number of meteorological stations capable of observing snowfall in QTP is limited and are primarily located to the eastern and southern part of the region. For future risk assessment, no projections of snow disaster events are provided in climate scenario datasets, although models have been developed to simulate daily snow depth (Yuan et al., 2016). Therefore, a snow disaster event identifier/simulator was developed here to identifying/simulating snow disasters.

A snow disaster is a weather process with snow fall, low temperature, and snow cover, with certain length of durations, according to the Chinese national standard for *Snow Disaster Grades in Grazing Regions of China* (GB/T20482-2017) and China Meteorological Administration (CMA) standard for *Meteorological Grades of Urban Snow Hazards* (QX/T 178-2013). A snow disaster event designation largely depends on the snow weather process and observer's decision (manual record). To mimic a meteorological observer's decision to designate a snow disaster event, our snow disaster event identifier/simulator has considered two major questions. First, whether a specific day would be regarded as a snow-disaster-day (SDD) given weather information of the day and previous days. The key is the modelling the binary response variables (Yes/No), which can be conducted with either regression or classification methods. Second, whether two SDDs, exactly neighbouring or a couple of days away from each other, should be regarded as one snow disaster event. The key is to assemble many single SDDs into snow disaster events, which can be accomplished using smoothing and filtering. In response, three major steps were considered (Fig. 2, Fig. A1):

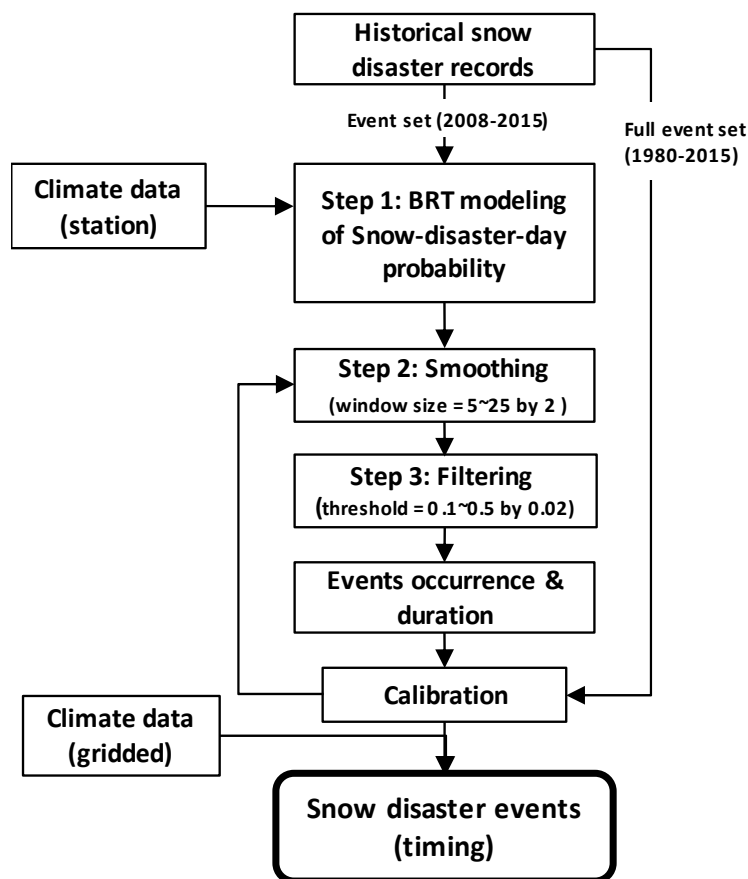


Fig. 2 Technical flow of the snow disaster event identifier/simulator

(1) Step 1: modelling the SDD probability for each single day

- 5 For this step, boosted regression tree (BRT) modelling was used to establish a multi-variate and non-linear relationship between SDD and various weather information. BRT modelling methodology was chosen due to its promising power for both explanatory and predictor purpose in many ecological and environmental modelling scenarios (Elith et al., 2008; Hastie et al., 2009). Other machine learning methods such as random forest can also be used here but less likely to outperform BRT according to the literature (Oppel et al., 2012; Youssef et al., 2016). To fit a BRT model, historical snow disasters were first
- 10 turned into SDD flags, if a date was included in a historical snow disaster it was flagged with “1”, and “0” otherwise. Variables used to explain and predict days that would be considered SDD was inspired by the two standards, GB/T20482-2017 and QX/T 178-2013. We included daily snow depth (*SD*, cm), daily maximum (*maxWind*), mean (*meanWind*) and minimum wind (*minWind*) speed (m/s), daily maximum (*maxT*), mean (*meanT*), and minimum (*minT*) temperature (°C), daily precipitation (*Pre*, mm), and average daily precipitation since the last snow fall day (precipitation > 0.1 mm) (*aveP*,



mm/d). Snow cover obtained from satellite imagery data was not considered because it is unavailable for future periods and predicting disasters, although, in this study, we used only historical data.

Historical snow disaster event data with the time of each event for each meteorological station were used to train the BRT model. These data were obtained from two sources. Records for 1980–2007 were obtained from W. Wang et al. (2013) while records from 2008–2015 were obtained from the China Meteorological Science Data Sharing Service System (CMSDS, <http://data.cma.gov.cn>). Data for the predictors were also obtained from CMSDS, including 106 national reference stations in the region. The dataset contains daily observations of maximum, mean and minimum temperature, maximum and mean wind speed, and precipitation.

BRT model fitting was conducted using the package *dismo* (Hijmans et al., 2011) in R 3.3.3. Given the type of response variable, the Bernoulli distribution family was used. To identify the best combination of model parameters, we compared the combinations of $lr = (0.01, 0.005, 0.001)$ and $tc = (1, 2, 3, 5)$, as recommended by Anderson *et al* (2016). The maximum number of trees was set to 10,000, which proved sufficient for convergence. For each combination of parameters, we applied the predictor selection process using the *gbm.simplify* function to best obtain a balance between prediction power and number of predictors requested. The result with the least cross-validation deviance was retained. To achieve the most promising goodness-of-fit, historical snow disaster records obtained from CMSDS (2008–2015) were used for fitting. This part of the data exactly matched the CMSDS record and most precisely followed CMA’s definition of a snow disaster. Records for 1980–2007 were used later for validation and calibration purposes.

(2) Steps 2 and 3: assembling single SDDs to events by smoothing and filtering

A fitted BRT model can help predict the probability of a single day being judged as a SDD. To predict/rebuild snow disaster events, these single day probabilities must be deemed snow disaster events, an ensemble of multiple SDDs. Because the explicit output from the BRT suffered from prediction errors, simply using a threshold to turn probabilities into “0/1” values would yield a set of “busy” snow disaster events, e.g., high frequency but small duration (Fig. A1, “Step 1”). Therefore, a smoothing treatment is needed to filter out isolated single SDDs and fill the small gaps between two neighbouring events. There are two parameters essential to changing the frequency and duration of identified snow disaster events: the smoothing window size and filtering threshold. In general, using larger window size for smoothing can filter out noises and reduce the frequency of events, while using lower threshold can increase the duration of single events. In order to best match the annual occurrence and the duration of single events, the two parameters were tuned through calibration using the full dataset of historical records between 1980 to 2015. We considered moving averages with window sizes from 5 d (minimum duration of a single disaster as defined by CMA) to 31 d (one month) in steps of 2 days, in combination with thresholds of 0.10 – 0.5 in steps of 0.02. The timing and duration of events derived from our model for any given pairs of window size and threshold were compared with historical records, including the frequency distribution of annual occurrence of single events, the frequency distribution of single event duration, and the timing of each single event. Through tuning, the combination of parameters that yielded the best matches were recorded.



Finally, the fitted BRT model together with the tuned parameters of smoothing and filtering was applied to generate all snow disaster events during 1980-2015 by grid. The China meteorological forcing dataset (He and Yang, 2011) obtained from the Scientific Data Centre of Cold and Arid Regions <http://westdc.westgis.ac.cn/data/7a35329c-c53f-4267-aa07-e0037d913a21> was used. It offers variables, including precipitation, air temperature, wind speed, and sunshine duration at spatial resolution of $0.1^\circ \times 0.1^\circ$ and temporal resolution of 3 h. We used this dataset because it focuses on the cold and arid regions in western China, and the QTP has been used as a focus region for validation (Chen et al., 2011; Yang et al., 2010). The 3-h dataset was aggregated to daily for input to the BRT model to rebuild gridded snow disaster events. Based on the identified events, the variables *Duration* and *Wind* were computed as inputs to the vulnerability function. From the 35 winters' events identified, we calculated the annual frequency and mean (single) event duration of snow disasters, as well as their return period values (Fig. A3).

2.3 Exposure

Exposure measures the distribution of assets or population exposed to hazards (Kinoshita et al., 2018). In our framework, it should provide the spatial distribution of herd size, and help turn the outputs from event loss modelling and livestock mortality rate (the response variable in the modelled vulnerability function) into mortality (death toll).

A full gridded distribution map of herd size in the QTP remains unavailable. The derivation of its spatial distribution was supported by the rule-of-thumb for “forage-livestock balance,” as written in the *Forage-livestock Balance Management Approach*. The *Approach* was issued by the Ministry of Agriculture of China in 2006 to mitigate severe over-grazing in the pastoral areas of China (Shang et al., 2012). Using the *Approach*, herd size at the county level was strictly controlled under carrying capacity computed according to a thorough investigation of local grassland resources. Therefore, a gridded carrying capacity map can be a good approximation of the actual herd size distribution.

We estimated the spatial distribution of herd size by turning grassland distribution data with the look-up table for grassland-type to carrying-capacity relationship. For the look-up table, we adapted the plan of Xin et al. (2011) for Qinghai and criteria outlined by the Land Management Administration of Tibet Autonomous Region (1994) for Tibet after reviewing various criteria (Zhang et al., 2014). For grassland distribution, we used the Vegetation Map of the People's Republic of China (1:1 million) (Editorial Committee of Vegetation Map of China, 2007), which offers detailed information about the spatial distribution of 11 vegetation type groups, 55 vegetation types, 960 plant formations, and more than 2000 dominant species in vector data. To match the look-up table and map information, we merged some vegetation types and used only the major grassland types (percentage area >0.5%) according to the FAO survey (2005) (Fig. A2; Table A1).

2.4 Loss modelling

Snow disaster event losses measured with livestock mortality rate (death toll/ herd size) were modelled by taking requested inputs into the vulnerability function. *Duration* and *Wind* were outputs from the hazard module. Growing season aggregate precipitation *P* was computed from the climate forcing data. For *GDP*, we used the fixed value for 2015 obtained from the



statistical year books of Qinghai, Tibet, Sichuan, Gansu, and Xinjiang. County level GDP values were assigned to each grid within its boundary. We used constant GDP values for 2015 for two reasons. First, the results can be directly treated as a stationary time series for estimating the probability distribution, as the influence of prevention capacity improvement has been removed. Second, it meets the goal of risk assessment, to estimate the likelihood of potential loss in the near future given present-day prevention capacity (prevention capacity equivalent to year 2015).

Event mortality rates were then aggregated into annual mortality rates, considering the possibility of multiple events per location annually, although unlikely. In aggregation, we assumed that the second snow disaster event can only have an impact on livestock surviving from the first event, and so on. Therefore, the annual aggregate loss rate in a given grid is

$$\Delta = 1 - \prod_{i=1}^N (1 - \delta_i), \quad i = 1, 2, \dots, N, \text{ in which } \delta_i \text{ is the modelled loss rate of the } i\text{th event in a year, and } N \text{ is the total number}$$

of events. The annual aggregate mortality rate can finally be turned into a death toll by multiplying exposure, the herd size in a given grid.

Event/annual mortality (death toll) can then be derived by multiplying event/annual loss rate in any given location by its herd size. For each grid, 35 annual loss records were modelled (there are 35 winters in 36 years), including both mortality and mortality rate figures. The number of event loss records differ by location, depending on the identified number of events for each grid.

2.5 Risk metrics

In the risk metrics, modelled losses of discrete event/annual losses were turned into probability distribution of losses. We followed standard risk metrics by deriving the average and return period values (Michel-Kerjan et al., 2013; Shi and Kasperson, 2015) of annual mortality rate and death toll for each grid. Due to our limited time span of repetition, return periods of 1/10 a (once in ten years, the 90th percentile of the distribution), 1/20 a, and 1/50 a were considered while 1/100 a usually used in flood/ earthquake studies (Kinoshita et al., 2018) was not considered. The kernel density method was employed to fit non-parametric distributions to derive those return period values by grid. We used the Gaussian kernel function and its corresponding optimal window width in the fitting process according to the “rule-of-thumb” for optimality (Deng et al., 2007; Silverman, 1986). In addition, aggregate mortality rate and death tolls at municipal level were also derived using zonal statistics, so as to better validate the result with historical losses, and provide policy implications.



3. Results

3.1 Model-predicted snow disaster duration

3.2.1 The trained BRT model and tuned parameters in rebuilding snow disaster events

The trained BRT model retained six variables but excluded *SD*, *minWind*, and *Pre*. In the final model, we used $lr = 0.001$ and $tc = 5$. It had a training data Area-Under-the-Curve (AUC) score of 0.858, and a cross-validation AUC of 0.829, indicating good predicting performance (Youssef et al., 2016). For the six variables entered in the final model (**Fig. 3**), *maxT* has the highest relative contribution (32.77%), while *meanWind* has the lowest (5.78%).

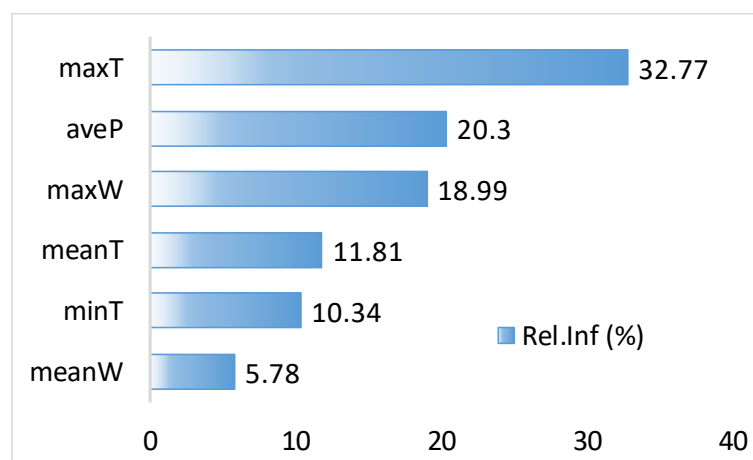


Fig. 3 Relative influence of variables predicting a snow-disaster-day. Blue bars are relative importance of each factor, and the sum of relative importance is 100%.

After tuning the window size with the moving average and threshold, we found the best results with a window size of 21 and a threshold of 0.18. The derived results well captured the timing of occurrence of historical events (**Fig. A1**) and matched the empirical cumulative density functions (ECDF) for historical durations (**Fig. 4**), for both event and annual aggregate durations. In historical records, two or more events in a single year at a single location are rare. Therefore, ECDFs for historical single event duration and annual aggregation duration were quite close to each other in Fig. 3. Two-sample Kolmogorov–Smirnov tests were also conducted to verify the degree of agreement between ECDFs. For single event duration (observed vs. predicted) the test statistics was 0.138, and its corresponding p-value was 0.118. The annual aggregate duration (observed vs. predicted) test statistics was 0.131, and its corresponding p-value was 0.189. Therefore, the prediction model well captured statistical features of historical snow disaster duration and the predicted results can be used for event loss modeling.

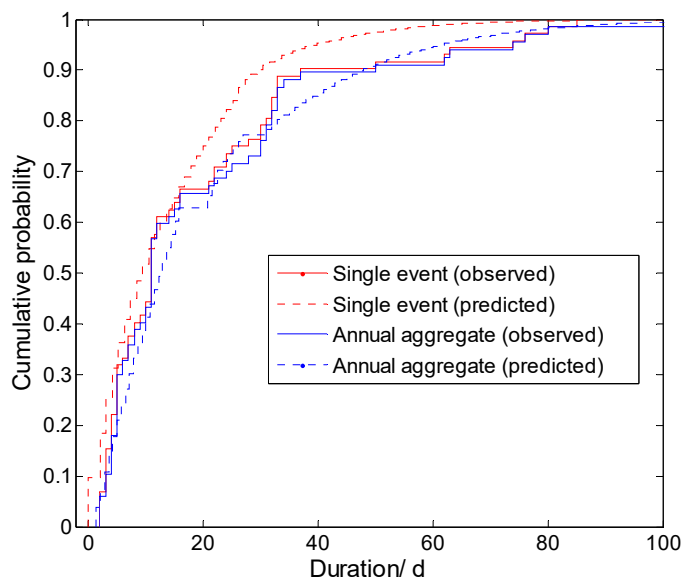


Fig. 4 Empirical cumulative density functions for historical and model-predicted snow disaster duration

3.2.1 Model-derived snow disaster events, 1980–2015

With the tuned model, the timing of snow disaster events were identified in the historical period 1980–2015. Correspondingly, the annual occurrence frequency and duration of snow disaster events were derived (Fig. 5). In the figure, non-grassland areas, including permanent snow areas, were masked using the vegetation map. Across the entire plateau, the annual average frequency was below 0.2 in most regions, i.e., on average, snow disasters occur every 5 years in these regions. Higher frequency regions were primarily located in major mountains, including the Tanggula Range and Nyainqêntanglha Range in the central part of the plateau, and the Kailas Range and neighboring Himalayas. These regions are higher elevation and spatially close to permanent snow-covered areas. For major pastoral production regions, i.e., the Naqu prefecture in the central QTP, the annual average frequency was 0.2 to 1, echoing the local proverb, “small disaster once in 3 years, and a major disaster once in 5 years” (Ye et al., 2017b).

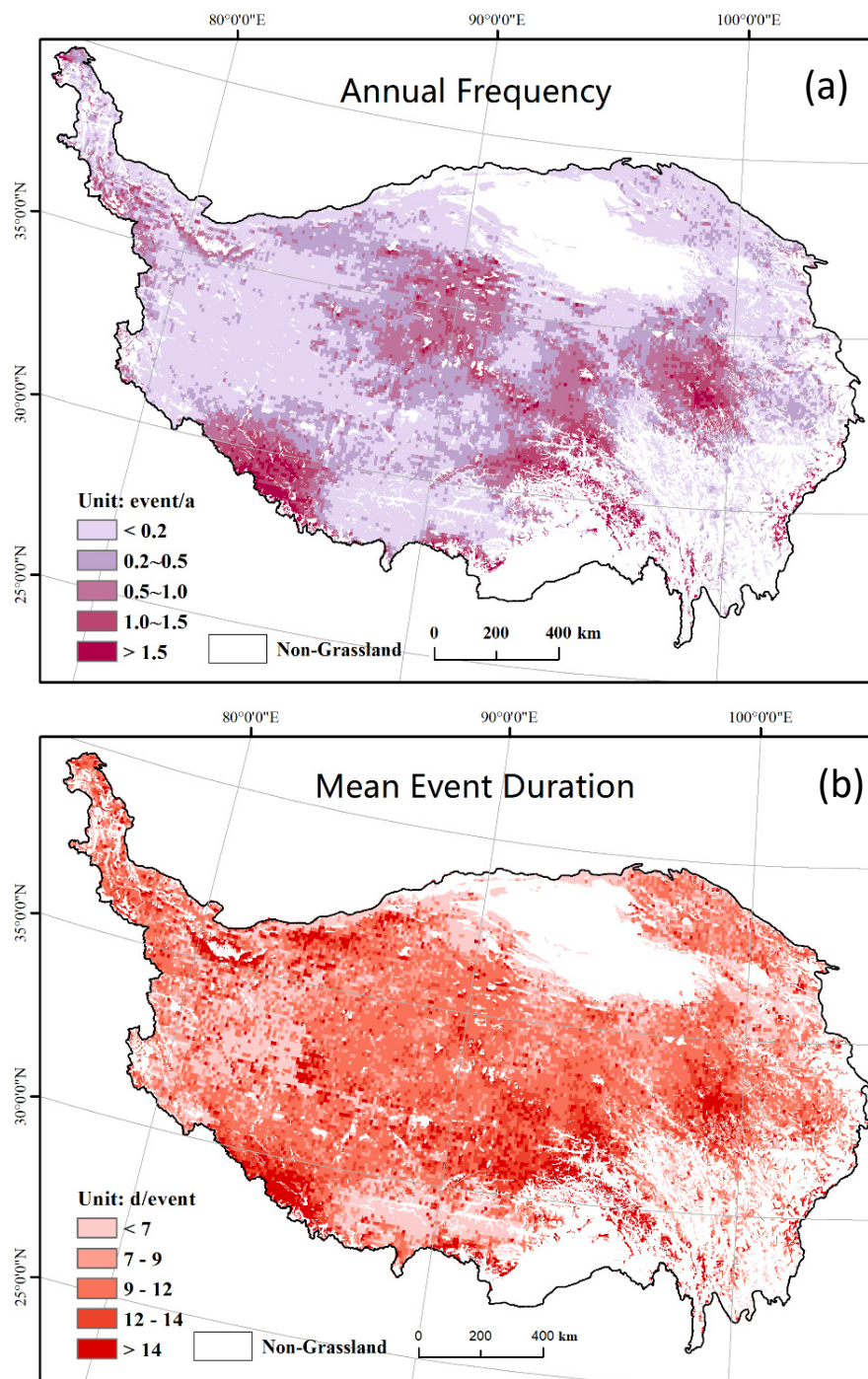


Fig. 5 Gridded annual frequency/ annual average occurrence (a) and mean event duration (b) of snow disasters from model predictions



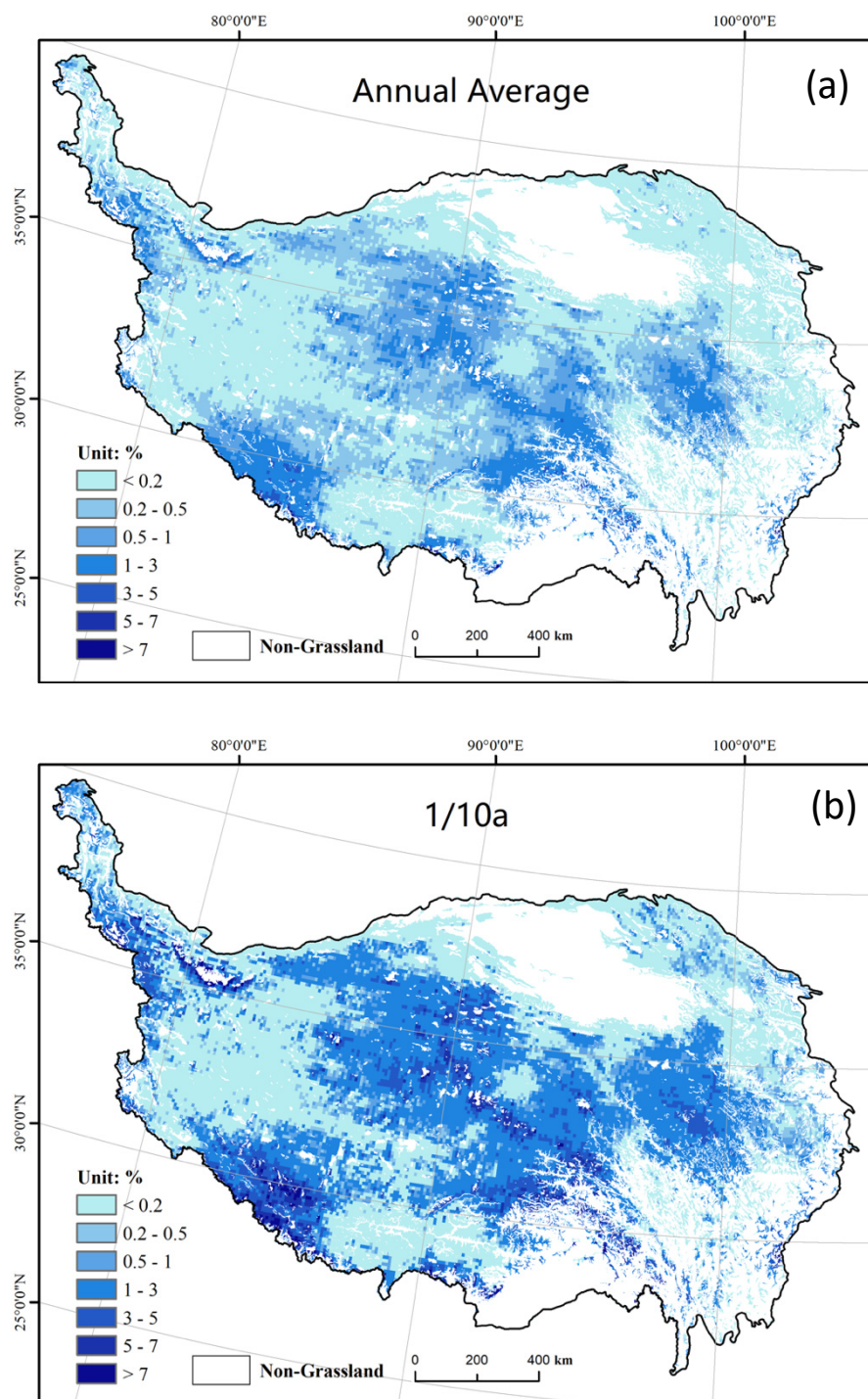
The distribution of mean event duration of snow disasters was consistent with annual frequency, indicating strong controls from elevation and topology. For most regions, mean event duration was below 7 d. For typical pastoral regions, i.e., Naqu Prefecture, a snow disaster can last for more than 12 d on average. Mean event duration can last for more than 14 d in high elevation mountainous areas, including the Himalayas in the southwest and alpine meadows to the east end of Bayankhar mountains, which is nearly 10% of the total grids with valid values.

3.2 Probabilistic risk assessment results

3.2.1 Risk in terms of livestock mortality rate

The assessed livestock snow disaster risk measured by annual mortality rate is presented in Fig. 6. As presenting the full probability distribution of livestock mortality rate by grid is not viable, these figures include the annual average and three return-period mortality rate maps (1/10a, 1/20a, and 1/50a), upon which the non-pasture areas were masked.

Spatial distributions of mortality rate at different return-periods are highly consistent (Fig. 6). The pattern is very similar to the pattern of annual aggregate snow disaster duration (Fig. 5), confirming the dominant influence of snow disaster duration. High-mortality rate regions are primarily located in the major mountainous areas, including the Tanggula Range and Nyainqêntanglha Range in the central QTP, the Kailas Range and neighboring Himalayas in the southwest QTP, Bayankhar mountains in the east QTP, and southern part of the Kalakoram Range and the west-end of the Kunlun Mountains in the northwest corner of the QTP. Classified by administrative districts, high mortality rate regions include the Yushu and Guoluo prefectures in Qinghai Province and Naqu, south Ngari, and Linzhi Prefectures in the Tibet Autonomous Region. In these regions, the annual average mortality rate ranges from 0.5% to 7.6%. The distribution of annual average mortality rate is extremely positively skewed. The cumulative percentage of grids with annual average mortality rates <0.5%, 1%, 2%, and 5% are 50%, 68%, 80%, and 98%, respectively. At return period of 1/20 a, estimated mortality rates range from 0.09% to 23%. The cumulative percentage of grids with 1/20 a mortality rates <0.5%, 1%, 2%, and 5% are 12%, 24%, 45%, and 89%, respectively.



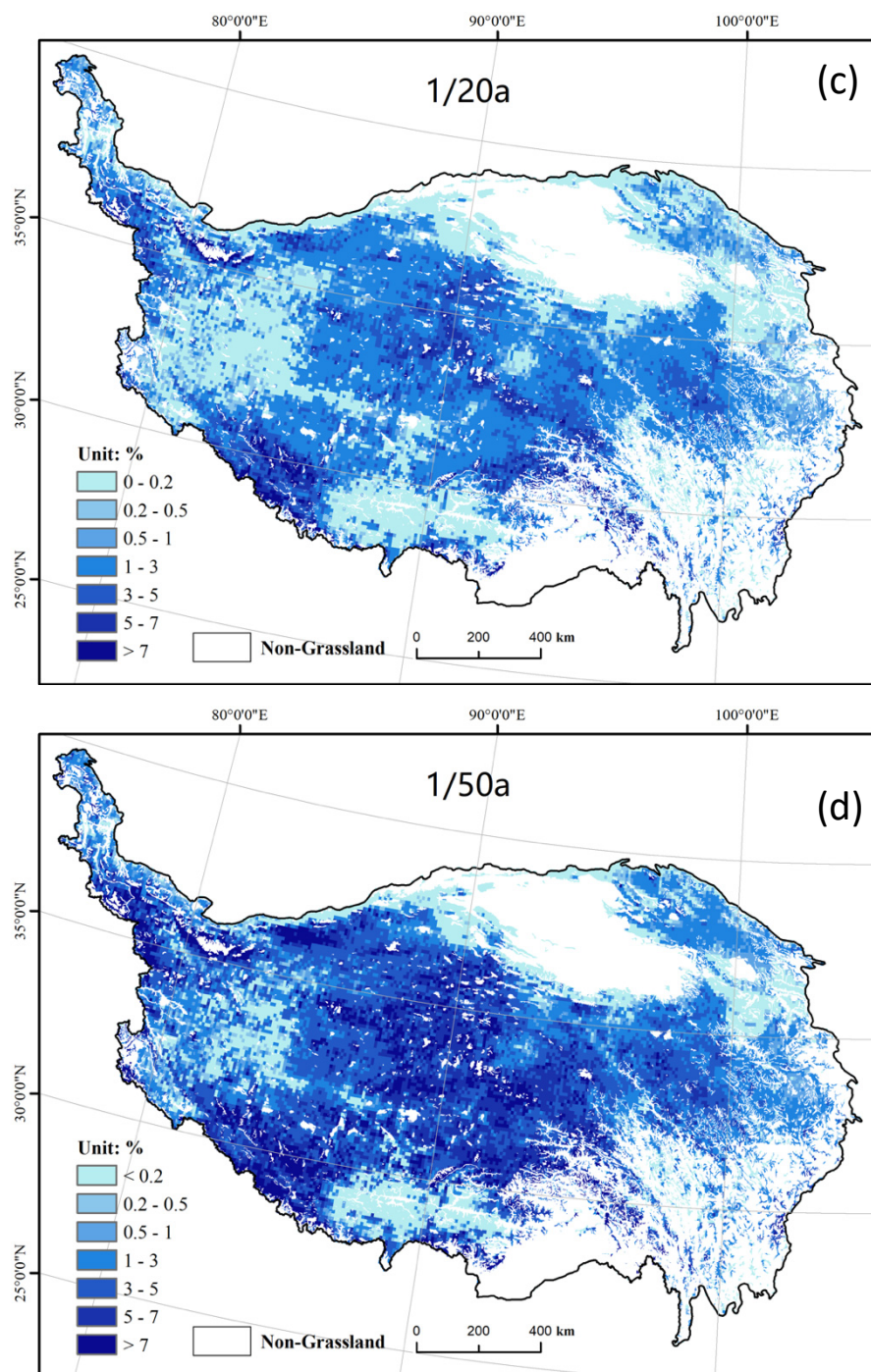
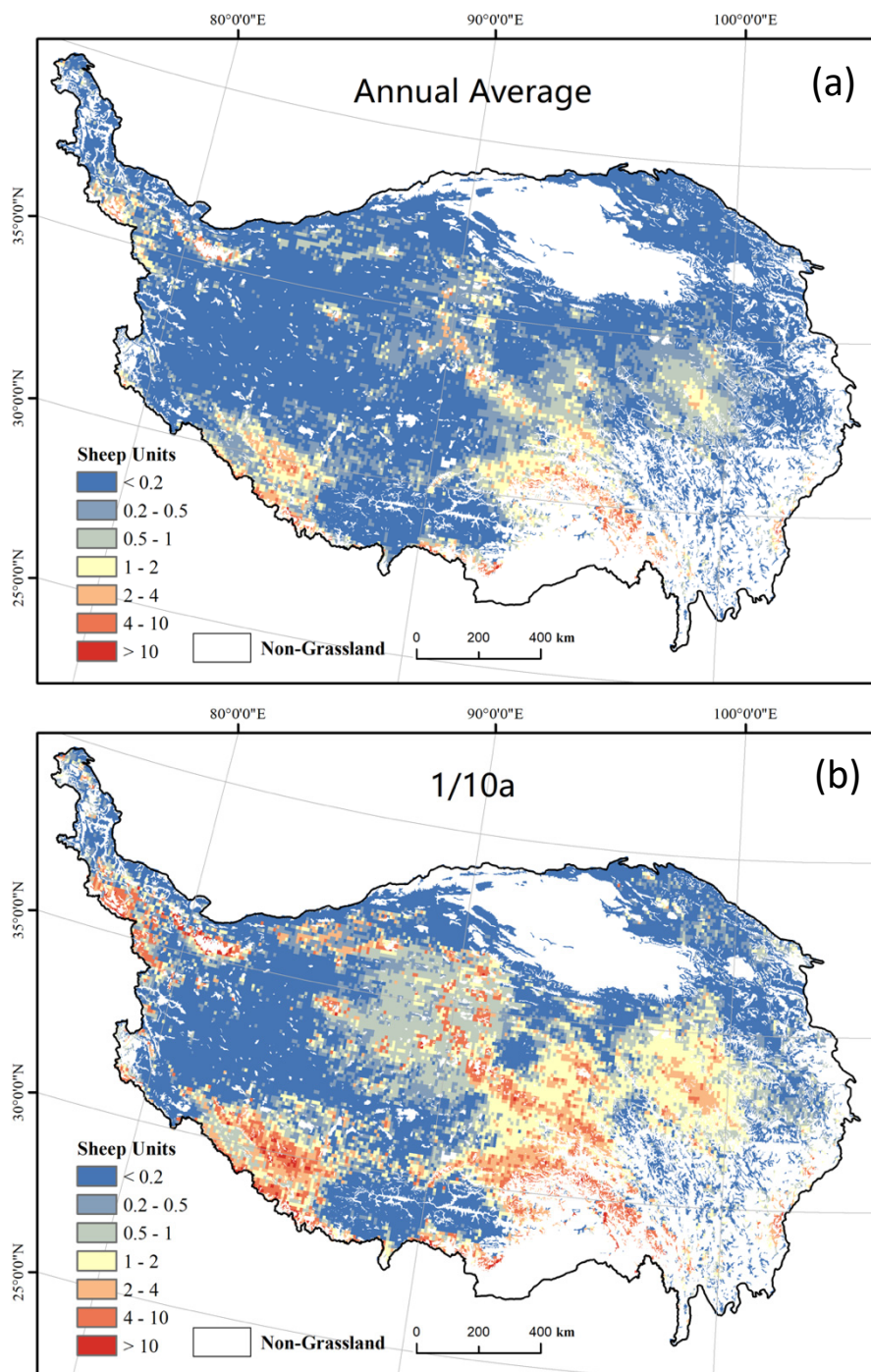


Fig. 6 Gridded livestock snow disaster risk in terms of mortality rate (%) in annual average values (a), and return-period values of 1/10a (b), 1/20a (c) and 1/50a (d). The grid size is $0.1^\circ \times 0.1^\circ$.



3.2.2 Risk in terms of livestock mortality

Risk metrics in terms of livestock mortality were then derived by multiplying the mortality rate by exposure (**Fig. 7**). Again, annual average mortality, and the mortality at 1/10 a, 1/20 a, and 1/50 a were all reported.



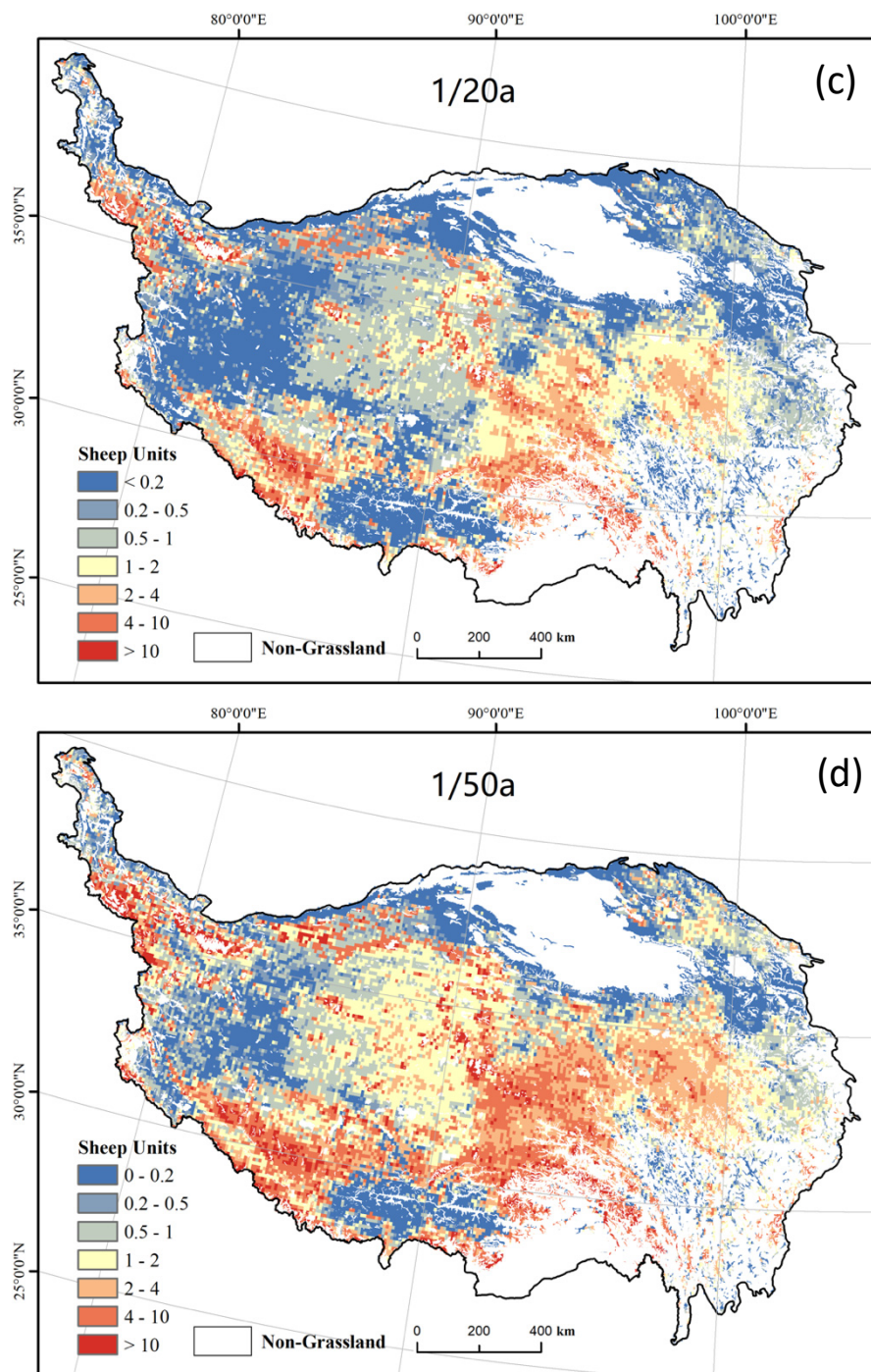


Fig. 7 Gridded livestock snow disaster risk in terms of mortality (sheep units) in annual average values (a), and return-period values of 1/10a (b), 1/20a (c) and 1/50a (d). The grid size is $0.1^\circ \times 0.1^\circ$.



The spatial distributions of snow disaster risk in terms of mortality across different return periods are generally in agreement. Again, the spatial pattern is very similar to that of mortality rate, indicating a relatively stronger influence from mortality rate than herd size. Regions of the highest risk (annual average mortality > 1 sheep units/km²) remain located in Nyainqêntanglha Range and the Kailas Range and neighboring Himalayas. The southern part of the Kalakoram Range and west-end of the Kunlun Mountains are also high risk areas. The Tanggula Range and Bayankhar mountains have relatively lower risk than the two regions mentioned above.

Mortality appears small in Fig. 7, mainly due to the herd size constrained by carrying capacity. When aggregated at the prefecture level, mortality remained considerable (Table 1). Zonal statistics results identified high risk prefectures, including Guoluo and Yushu in Qinghai Province and Naqu, Shigatse, Changdu, and Nagri in Tibet Autonomous Region. In these prefectures annual mortality with a return period of 1/20 a was mostly greater than 100,000 sheep units (the threshold for a severe livestock snow disaster, as defined in GB/T20482-2017). Among them, Yushu, Naqu, Shigatse, and Nagri are of extremely high risk. Their 1/20 a mortality was all $> 200,000$ sheep units (the threshold for an extremely severe livestock snow disaster, as defined in GB/T20482-2017).

Table 1 Livestock snow disaster risk in terms of mortality (1,000 sheep units) by prefecture

Prefecture	Herd size (estimated)	Mortality (annual average)	Mortality (1/20 a)	Mortality (1/50 a)
Xining	283.4	0.1	0.8	2.1
Haidong	437.2	0.2	1.0	2.1
Haibei	2036	1.9	13.3	26.6
Huangnan	1080.2	1.0	6.1	13.1
Hainan	1692.7	1.4	8.0	16.9
Guoluo	5160.7	32.2	111.7	170.6
Yushu	12720.9	69.0	305.8	535.6
Haixi	10659.2	32.5	45.3	102.0
Lahsa	1802.1	9.0	41.2	85.3
Changdu	4217.4	70.8	188.8	281.8
Shannan	2607.5	32.7	89.7	142.8
Shigatse	12245.4	117.1	393.9	608.9
Naqu	17877.2	129.2	530.1	956.7
Ngari	12970.8	47.3	243.6	504.6
Linzhi	2743.9	101.2	244.4	339.3

Note: Only prefectures with a majority of land mass within the QTP are listed. Statistics reported in the table only refer to areas within the QTP.



4. Discussion

4.1 Spatial patterns of livestock snow disaster risk in the QTP

Our results illustrate the spatial distribution and offer quantitative metrics of risk in terms of livestock mortality and mortality rate due to snow disasters in the QTP. The spatial pattern of risk agrees with earlier studies covering this region quite well. From an empirical perspective, the literature frequently mentions Easter Inner Mongolia, the Northern Tianshan Mountains in Xinjiang, and Northeastern QTP as centers of snow disaster around China (Gao, 2016; Hao et al., 2002). Within the QTP, high frequency snow disaster regions that are mentioned repeatedly in the literature include Yushu, Guoluo, Naqu, Shigates, and Nagri (Bai et al., 2011), which have all been identified in our study. As for risk assessment, our results also agree well with earlier studies. For instance, regions between the Kailas Range and neighboring Himalayas, southern Qinghai Province (mainly Yushu and Guoluo), and the northwestern corner of the QTP are all considered as higher risk regions in both qualitative (Liu et al., 2014b) and quantitative (Shi, 2011; p.106-107) risk assessment results. In northern and western Naqu Prefecture, and the central-to-western end of the Nyainqêntanglha Range, our results are consistent with the national snow disaster risk map (Shi, 2011; hereafter termed risk maps), which are of higher-to-the-highest risk. Nevertheless, these regions are considered the lowest of lower risk in the results presented by Fenggui Liu et al. (2014).

For the magnitude of annual average mortality rate, our results were smaller than those in the risk maps of China (Shi, 2011; p.104-107); in general, our results had values about half those previously reported. For the high-risk regions, annual average mortality rates were generally $\geq 2\%$ in our results, but $\geq 4\%$ in the risk map results. Our result had a vast low risk region with annual average mortality rates $<0.5\%$, but the threshold was $1\sim 3\%$ in the risk maps. In terms of mortality, our results matched historical records better. For instance, the most severe snow disaster in southern Qinghai Province since 1960 was in 1996, mostly in Guoluo and Yushu (Bai et al., 2011), the deadliest disaster in nearly 65 years. It claimed a loss of 1.08 million livestock (equivalent to $1.5\sim 2 \times 10^6$ sheep units, assuming the local herd structure for 2016). According to our risk metrics, an annual loss of 2×10^6 (summing Guoluo and Yushu) would have a return period over 100 years (Table 2). Another example is the 1997–1998 snow disaster in Naqu, the most severe snow disaster since 1960, leading to a loss of 0.82×10^6 livestock (equivalent to have 1.2×10^6 sheep units, assuming the local herd structure for 2016) (Wen, 2008). Again, an annual loss of 1.2×10^6 sheep units has a return period of 50 to 70 years according to our metrics. As we have assumed stronger prevention capacity using the GDP values for 2015, it is natural to have a higher return period than empirical values. If the mortality rate estimated in risk maps were used instead, then the corresponding return-period could be underestimated by approximately 1/20 a, and consequently, snow disaster risk would be exacerbated.

4.2 Advantages of the event-based PRA

Our study differ from the existing literature largely in its event-based PRA framework. Such a framework derives unique information that can hardly be obtained by earlier methods that are based on annual basis, which are important for preparedness decisions and insurance solutions. For instance, the event-based framework enables the estimation of frequency



distribution of the occurrence and duration of single disaster events. Overall, our analysis indicates that snow disasters are frequent in terms of annual occurrence but more than one snow disaster a year is unlikely (Fig. 5). Given this finding, prior counter-measures should be implemented to build prevention capacity to handle the one event in every year (Mechler et al., 2010).

5 Our results for single event duration provide important quantitative references for hay and fodder storage, which were not achieved by earlier annual basis analyses. For the majority of higher-risk regions, once a snow disaster occurred, on average it lasted for 12 d (Fig. 5). At return periods of 1/10 a and 1/20 a, the durations of single events were up to 21 days and 28 days, respectively (Fig. A2). At return periods of 1/50 a, single events could even last for more than 40–50 days. The regional average duration of a 1/20 a event in Naqu, Yushu, Guoluo, and south Ngari, was estimated to be 24, 22, 26, and 26
 10 days, respectively. From a preparedness perspective, the amount of hay and fodder storage needed, from combined herder households and local government reserves, can be readily estimated from our results once their goal of preparedness capacity is set, i.e., capable of managing a 1/10 a event. Alternatively, our results can also help local regions measure their preparedness capacity given their amount of hay and fodder storage.

Our event-based PRA results also provide solid technical support for insurance solutions. Earlier studies that assess risk on
 15 annual basis using annual aggregate snow-cover days, or snow depth variables are not capable of doing so as insurance indemnities must be clearly triggered by specific events. The capability of finding the frequency distribution of event occurrence and event duration provides necessary information to help the design of insurance trigger schemes. Meanwhile, our results can readily support the calculation of actuarially fair premium rates and cat-risk loadings by applying deductible conditions to turn event loss records into event-based insurance losses, and then calculating annual average and return period
 20 insurance loss-cost ratios (Wang and Zhang, 2003).

4.3 Risk-informed implications

Our results imply that the present level of preparedness in local regions are far from sufficient. According to our local survey data, a sheep unit, even under the minimum level of supplementary feeding, consumes 1 kg of hay and 0.5 kg of fodder (Ye et al., 2017b). Nyainrong County in central Naqu Prefecture prepared a 4.4-million yuan fund to prepare winter storage of
 25 hay and fodder in 2016. The total amount of hay bought (460 ton) can only support supplementary feeding of county-wide livestock (1167.6 thousand sheep units) for at most 3~5 days. Such a level of preparedness can only endure a snow disaster with return period less than 1/5 a. This discrepancy also explains the frequent losses from snow disasters in these regions.

It is not straightforward to improve such preparation capacity to manage higher return-period events. As the herd size has mostly reached the defined carrying capacity, hay harvests for winter seasons from local grassland are much less feasible
 30 (Shang et al., 2012). Agro-pastoral regions, i.e., the northeast, southeast, and southern parts of the QTP, mostly the agro-pastoral regions in Qinghai, Gansu, Sichuan, and Shigatse in Tibet, can obtain some support from crop straws. Pure pastoral regions, i.e., Naqu and Nagri, are problematic, due to the lack of local resources, and the high transportation cost to import from other regions. To enhance preparedness capacity, inter-prefecture overall planning will be needed to arrange support



- from agro-pastoral regions, e.g. Shigatse and Lhasa, to pastoral regions. In addition, forage harvesting bases within small parts of pastoral regions with relatively large precipitation and grassland productivity will also be favoured. However, it remains less likely that local regions will be able to provide sufficient hay and fodder to endure long-lasting events, i.e. > 14 d or an equivalent event with a return period larger than 10 a.
- 5 Due to the difficulty in improving prevention capacity, insurance schemes are needed to provide relief (Mechler et al., 2010). The insurance product could be conventional (indemnity-based), where the post-disaster loss-adjustment is conducted on herder household bases. A more favourable choice is to adopt an index-based structure using livestock mortality rate as predicted by our model, in which disaster duration and growing season aggregate precipitation are two critical indices. The index-based structure is much more efficient in vast and sparsely populated regions by expediting the loss-adjustment
 - 10 process, and consequently, should save considerable associated costs (Ye et al., 2017b). Furthermore, using a model-predicted mortality rate can encourage local communities to invest in prevention and preparedness, and reduce moral hazards (Miranda and Farrin, 2012).

4.4 Limitations

- Several limitations in our risk assessment model must be mentioned. First, our hazard module to rebuild/predict snow
- 15 disaster still suffers from uncertainty. We obtained a good AUC score from the BRT model for identifying snow disaster days, and also good agreement in timing of occurrence and distribution of duration for longer-duration events. However, the performance in capturing small disasters of short-duration, i.e., < 5 d, still needs improvement.

- Due to the lack of exact spatial distribution of sheep units, the exposure data was derived according to the computed carrying capacity by grassland types. The total herd sizes computed differ within 20% to those reported in the statistical yearbooks at
- 20 the prefecture levels for pastoral regions. The difference for agro-pastoral prefectures in the eastern QTP was much larger, as agriculture provides extra foodstuff for raising livestock and supports livestock farms in addition to free grazing. Fortunately, as snow disaster threats have little impact on livestock kept on farms, our result is less likely to severely underestimate mortality in these locations. For prefectures in the central and western part of the region, our result is of practical significance for use as a reference for livestock mortality under the long-run forage-livestock balance, irrespective of the
 - 25 present true herder size.

Finally, our risk metrics were derived from events rebuilt from historical climate data, but not from stochastic simulations. Consequently, we have a limited number of events and annual loss records. We are only confident for risk metrics less than 1/35 a. Metrics for any higher return periods were derived from extrapolation and must be used with caution. This limitation can be resolved by inputting stochastic climate datasets using a stochastic weather simulator.



5. Conclusions

Quantitative risk metrics derived under a probabilistic risk assessment framework are critical for understanding disaster risks and providing quantitative evidence for risk-informed decision-making and resilience-building. In this study, we developed an event-based PRA approach for livestock snow disaster in the QTP region and derived risk metrics for livestock mortality and mortality rate. Our assessment results show that the spatial distributions for mortality rate and mortality size are quite similar. Hazard intensity, in terms of disaster duration, was the major driver of spatial differences in livestock mortality, while the influence from exposure in terms of herd size was quite modest. High risk regions include the Nyainqêntanglha Range, Tanggula Range, Bayankhar mountains, and the region between the Kailas Range and neighboring Himalayas. At a return period of 1/20 a, the annual livestock mortality rate was estimated to be $> 2\%$ and mortality was estimated to be > 2 sheep unit/km². At prefecture levels, the most important animal husbandry bases were identified as high risk regions, including Guoluo and Yushu in Qinghai Province and Naqu, Shigatse, Changdu, and Nagri in the Tibet Autonomous Region. In these prefectures, a snow disaster event with return period of 1/20 a or higher can easily claim a total loss of more than 100,000 sheep units. Our results of return-period mortality rate and death toll show better agreement with historical losses than those reported earlier.

Compared to earlier results, our approach relies on the prediction/simulation of snow disaster events, and correspondingly the modelled livestock losses are on event basis. In addition, our quantitative results for the return-period disaster duration are valuable for preparing hay and fodder reserves and designing insurance protection. The methodology developed here can be further adapted to future climate change risk analysis and providing risk-informed adaption suggestions for the QTP region.

Acknowledgements

This study was supported by the National Key R&D Program of China (grant number 2016YFA0602404), the Fund for Creative Research Groups of the National Natural Science Foundation of China (grant number 41621061), and the State Key Laboratory of Earth Surface Processes and Resource Ecology.

References

Anderson, D., Davidson, R. A., Himoto, K. and Scawthorn, C.: Statistical Modeling of Fire Occurrence Using Data from the Tōhoku, Japan Earthquake and Tsunami, *Risk Anal.*, 36(2), 378–395, doi:10.1111/risa.12455, 2016.



- Bai, Y., Zhang, X. and Xu, P.: The Snow Disaster Risk Assessment of Animal Husbandry in Qinghai Province, J. Qinghai Norm. University(Nat. Sci., (1), 71–77, doi:10.16229/j.cnki.issn1001-7542.2011.01.004, 2011.
- Birkmann, J. and Welle, T.: The WorldRiskIndex 2016: Reveals the Necessity for Regional Cooperation in Vulnerability Reduction, J. Extrem. Events, 3(2), 1650005, doi:10.1142/S2345737616500056, 2016.
- 5 Carleton, T. A. and Hsiang, S. M.: Social and economic impacts of climate, Science (80-.), 353(6304), doi:10.1126/science.aad9837, 2016.
- Chen, Y., Yang, K., He, J., Qin, J., Shi, J., Du, J. and He, Q.: Improving land surface temperature modeling for dry land of China, J. Geophys. Res. Atmos., 116(20), doi:10.1029/2011JD015921, 2011.
- Deng, X., Barnett, B. J. and Vedenov, D. V.: Is There a Viable Market for Area-Based Crop Insurance?, Am. J. Agric. Econ., 10 89(2), 508–519, doi:10.1111/j.1467-8276.2007.00975.x, 2007.
- Editorial Committee of Vegetation Map of China, C. A. of S.: Vegetation Map of the People’s Republic of China (1:1000000), 2007.
- Elith, J., Leathwick, J. R. and Hastie, T.: A working guide to boosted regression trees, J. Anim. Ecol., 77(4), 802–813, doi:10.1111/j.1365-2656.2008.01390.x, 2008.
- 15 Fang, Y., Zhao, C., Ding, Y., Qin, D. and Huang, J.: Impacts of snow disaster on meat production and adaptation : an empirical analysis in the yellow river source region, Sustain. Sci., 11(2), 249–260, doi:10.1007/s11625-015-0325-5, 2016.
- FAO: Grassland of the World, Accessed, <http://www.fao.org/docrep/008/y8344e/y8344e05.htm> [online] Available from: <http://www.fao.org/docrep/008/y8344e/y8344e08.htm>, 2005.
- Fernández-Giménez, M. E., Batkhishig, B. and Batbuyan, B.: Cross-boundary and cross-level dynamics increase 20 vulnerability to severe winter disasters (dzud) in Mongolia, Glob. Environ. Chang., 22(4), 836–851, doi:10.1016/j.gloenvcha.2012.07.001, 2012.
- Fernández-Giménez, M. E., Batkhishig, B., Batbuyan, B. and Ulambayar, T.: Lessons from the Dzud: Community-Based Rangeland Management Increases the Adaptive Capacity of Mongolian Herders to Winter Disasters, World Dev., 68(1), 48–65, doi:10.1016/j.worlddev.2014.11.015, 2015.
- 25 Gao, J.: Analysis and assessment of the risk of snow and freezing disaster in China, Int. J. Disaster Risk Reduct., 19, 334–340, doi:10.1016/J.IJDRR.2016.09.007, 2016.
- Hao, L., Wang, J., Man, S. and Yang, C.: Spatio-temporal change of snow disaster and analysis of vulnerability of animal husbandry in China, J. Nat. Disasters, 11(4), 42–48, 2002.
- Hastie, T., Tibshirani, R. and Friedman, J.: The Elements of Statistical Learning, Elements, 1, 337–387, doi:10.1007/b94608, 30 2009.
- He, J. and Yang, K.: China Meteorological Forcing Dataset, Cold Arid Reg. Sci. Data Cent. Lanzhou, 2011, doi:10.3972/westdc.002.2014.db, 2011.
- Hijmans, R. J., Phillips, S., Leathwick, J. R. and Elith, J.: Package “dismo,” R Packag., 55, doi:10.1016/j.jhydrol.2011.07.022., 2011.



- Jongman, B., Winsemius, H. C., Aerts, J. C. J. H., Coughlan de Perez, E., van Aalst, M. K., Kron, W. and Ward, P. J.: Declining vulnerability to river floods and the global benefits of adaptation., *Proc. Natl. Acad. Sci. U. S. A.*, 112(18), E2271-80, doi:10.1073/pnas.1414439112, 2015.
- Kinoshita, Y., Tanoue, M., Watanabe, S. and Hirabayashi, Y.: Quantifying the effect of autonomous adaptation to global river flood projections: application to future flood risk assessments, *Environ. Res. Lett.*, 13(1), 014006, doi:10.1088/1748-9326/aa9401, 2018.
- Land Management Administration of Tibet Autonomous Region: Grassland Resources in the Tibet Autonomous Region, Science Press, Beijing., 1994.
- Li, F., Hou, G., E, C., Liu, Z., Jiang, Y. and Xi, Y.: Township unit-based risk assessment of snowstorm hazard in Guoluo Prefecture of Qinghai Plateau, *J. Nat. Disasters*, 141–148, 2014.
- Li, Y., Ye, T., Liu, W. and Gao, Y.: Linking livestock snow disaster mortality and environmental stressors in the Qinghai-Tibetan Plateau: Quantification based on generalized additive models, *Sci. Total Environ.*, 625(12), 87–95, doi:10.1016/j.scitotenv.2017.12.230, 2018.
- Liu, F., Mao, X. and Zhang, Y.: Risk analysis of snow disaster in the pastoral areas of the Qinghai-Tibet Plateau, *Geogr. Sci.*, 411, 2014a.
- Liu, F., Mao, X., Zhang, Y., Chen, Q., Liu, P. and Zhao, Z.: Risk analysis of snow disaster in the pastoral areas of the Qinghai-Tibet Plateau, *J. Geogr. Sci.*, 24(3), 411–426, doi:10.1007/s11442-014-1097-z, 2014b.
- Mechler, R., Hochrainer, S., Pflug, G., Lotsch, A. and Williges, K.: Assessing the Financial Vulnerability to Climate-Related Natural Hazards. [online] Available from: <https://ssrn.com/abstract=1565993> (Accessed 20 May 2018), 2010.
- Michel-Kerjan, E., Hochrainer-Stigler, S., Kunreuther, H., Linnerooth-Bayer, J., Mechler, R., Muir-Wood, R., Ranger, N., Vaziri, P. and Young, M.: Catastrophe risk models for evaluating disaster risk reduction investments in developing countries., *Risk Anal.*, 33(6), 984–99, doi:10.1111/j.1539-6924.2012.01928.x, 2013.
- Miranda, M. J. and Farrin, K.: Index Insurance for Developing Countries, *Appl. Econ. Perspect. Policy*, 34(3), 391–427, doi:10.1093/aepp/pps031, 2012.
- Muis, S., Güneralp, B., Jongman, B., Aerts, J. C. J. H. and Ward, P. J.: Flood risk and adaptation strategies under climate change and urban expansion: A probabilistic analysis using global data, *Sci. Total Environ.*, 538, 445–457, doi:10.1016/J.SCITOTENV.2015.08.068, 2015.
- Oppel, S., Meirinho, A., Ramírez, I., Gardner, B., O’Connell, A. F., Miller, P. I. and Louzao, M.: Comparison of five modelling techniques to predict the spatial distribution and abundance of seabirds, *Biol. Conserv.*, 156, 94–104, doi:10.1016/J.BIOCON.2011.11.013, 2012.
- Shang, Z. H., Gibb, M. J. and Long, R. J.: Effect of snow disasters on livestock farming in some rangeland regions of China and mitigation strategies - A review, *Rangel. J.*, 34(1), 89–101, doi:10.1071/RJ11052, 2012.
- Shi, P. and Kasperson, R. E.: World Atlas of Natural Disaster Risk, Beijing Normal University Press and Springer, Beijing., 2015.



- Shi, P.: Atlas of Natural Disaster Risk of China, edited by P. Shi, Scientific Press, Beijing, Beijing., 2011.
- Silverman, B.: Density estimation for statistics and data analysis., 1986.
- Sternberg, T.: Investigating the presumed causal links between drought and dzud in Mongolia, *Nat. Hazards*, 1–17, doi:10.1007/s11069-017-2848-9, 2017.
- 5 Tachiiri, K. and Shinoda, M.: Quantitative risk assessment for future meteorological disasters: Reduced livestock mortality in Mongolia, *Clim. Change*, 113(3–4), 867–882, doi:10.1007/s10584-011-0365-5, 2012.
- Tachiiri, K., Shinoda, M., Klinkenberg, B. and Morinaga, Y.: Assessing Mongolian snow disaster risk using livestock and satellite data, *J. Arid Environ.*, 72(12), 2251–2263, doi:10.1016/j.jaridenv.2008.06.015, 2008.
- UNISDR: Sendai Framework for Disaster Risk Reduction 2015 - 2030, in Third World Conference on Disaster Risk Reduction, Sendai, Japan, 14-18 March 2015., pp. 1–25., 2015.
- 10 Wang, H. H. and Zhang, H.: On the Possibility of a Private Crop Insurance Market: A Spatial Statistics Approach, *J. Risk Insur.*, 70(1), 111–124, doi:10.1111/1539-6975.00051, 2003.
- Wang, J., Brown, D. G. and Agrawal, A.: Climate adaptation, local institutions, and rural livelihoods: A comparative study of herder communities in Mongolia and Inner Mongolia, China, *Glob. Environ. Chang.*, 23(6), 1673–1683, doi:10.1016/j.gloenvcha.2013.08.014, 2013a.
- 15 Wang, J., Wang, Y. and Wang, S.: Biophysical and socioeconomic drivers of the dynamics in snow hazard impacts across scales and over heterogeneous landscape in Northern Tibet, *Nat. Hazards*, 81(3), 1499–1514, doi:10.1007/s11069-015-2142-7, 2016.
- Wang, W., Liang, T., Huang, X., Feng, Q., Xie, H., Liu, X., Chen, M. and Wang, X.: Early warning of snow-caused disasters in pastoral areas on the Tibetan Plateau, *Nat. Hazards Earth Syst. Sci.*, 13(6), 1411–1425, doi:10.5194/nhess-13-1411-2013, 2013b.
- Wang, Y., Wang, J., Li, S. and Qin, D.: Vulnerability of the Tibetan pastoral systems to climate and global change, *Ecol. Soc.*, 19(4), doi:10.5751/ES-06803-190408, 2014.
- Wei, Y., Wang, S., Fang, Y. and Nawaz, Z.: Integrated assessment on the vulnerability of animal husbandry to snow disasters under climate change in the Qinghai-Tibetan Plateau, *Glob. Planet. Change*, 157(March), 139–152, doi:10.1016/j.gloplacha.2017.08.017, 2017.
- 25 Wen, K.: China meteorological disasters catalog, Meteorological Press, Beijing., 2008.
- Wu, J., Li, N., Yang, H. and Li, C.: Risk evaluation of heavy snow disasters using BP artificial neural network: the case of Xilingol in Inner Mongolia, *Stoch. Environ. Res. Risk Assess.*, 22(6), 719–725, doi:10.1007/s00477-007-0181-7, 2007.
- 30 Xin, Y., Du, T., Xin, Y., Wu, A. and Lu, F.: The Evaluation of Carrying Capacity of Grassland in Qinghai, *Qinghai Prataculture*, 20(4), 13–22, 2011.
- Yang, K., He, J., Tang, W., Qin, J. and Cheng, C. C. K.: On downward shortwave and longwave radiations over high altitude regions: Observation and modeling in the Tibetan Plateau, *Agric. For. Meteorol.*, 150(1), 38–46, doi:10.1016/j.agrformet.2009.08.004, 2010.



- Ye, T., Li, Y., Gao, Y., Wang, J. and Yi, M.: Designing index-based livestock insurance for managing snow disaster risk in Eastern Inner Mongolia, China, *Int. J. Disaster Risk Reduct.*, 23(April), 160–168, doi:10.1016/j.ijdr.2017.04.013, 2017a.
- Ye, T., Li, Y.J., Shi, P.J., Liu, W.H., 2018. Quantifying livestock vulnerability to snow disasters in the Tibetan Plateau: comparing different modeling techniques for prediction. *Glob. Planet. Change* (Under review)
- 5 Ye, T., Wu, J., Li, Y. and Gao, Y.: Designing index-based livestock insurance for managing snow disaster risk in the central Qinghai–Tibetan Plateau. Research Report Funded by the International Center for Collaborative Research on Disaster Risk Reduction (ICCR-DRR)., 2017b.
- Yin, H., Cao, C., Xu, M., Chen, W., Ni, X. and Chen, X.: Long-term snow disasters during 1982–2012 in the Tibetan Plateau using satellite data, *Geomatics, Nat. Hazards Risk*, 8(2), 466–477, doi:10.1080/19475705.2016.1238851, 2017.
- 10 Youssef, A. M., Pourghasemi, H. R., Pourtaghi, Z. S. and Al-Katheeri, M. M.: Landslide susceptibility mapping using random forest, boosted regression tree, classification and regression tree, and general linear models and comparison of their performance at Wadi Tayyah Basin, Asir Region, Saudi Arabia, *Landslides*, 13(5), 839–856, doi:10.1007/s10346-015-0614-1, 2016.
- Yuan, W., Xu, W., Ma, M., Chen, S., Liu, W. and Cui, L.: Improved snow cover model in terrestrial ecosystem models over the Qinghai-Tibetan Plateau, *Agric. For. Meteorol.*, 218–219, 161–170, doi:10.1016/j.agrformet.2015.12.004, 2016.
- 15 Zhang, Y. J., Zhang, X. Q., Wang, X. Y., Liu, N. and Kan, H. M.: Establishing the carrying capacity of the grasslands of China: A review, *Rangel. J.*, 36(1), 1–9, doi:10.1071/RJ13033, 2014.



Appendix

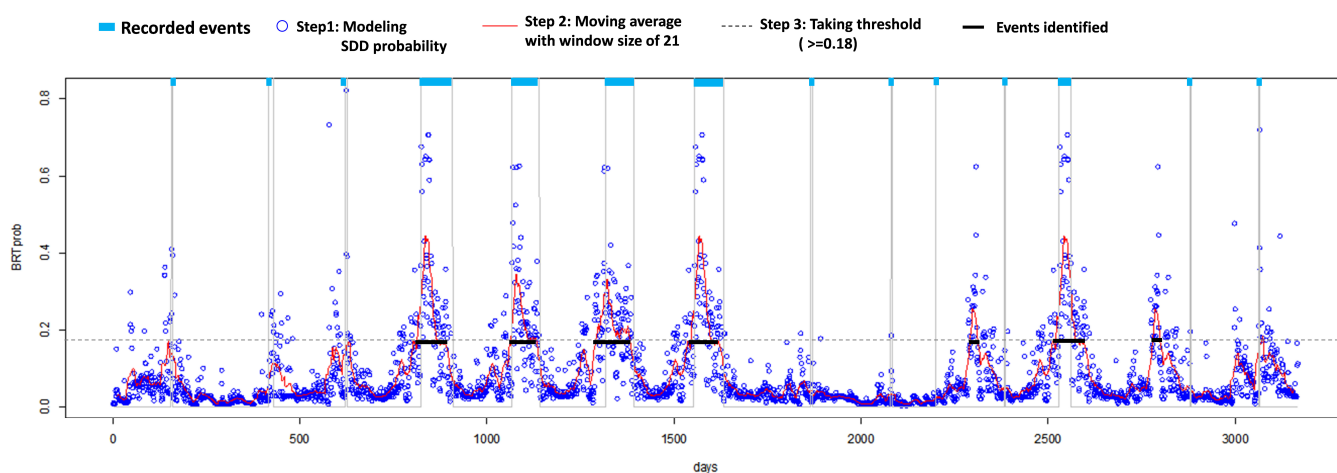


Fig. A1 Illustrative chart of the procedure for identifying snow disaster events, and its calibration with historical records. The time series is the conjunction of days in the winter season (October 1 to May 31) with snow disaster records after 2008. In total, this includes 13 station•winter and 3168 single days. The figure shows that the procedure is capability of accurately capturing major historical events with relatively longer duration in terms of both timing of occurrence and duration.

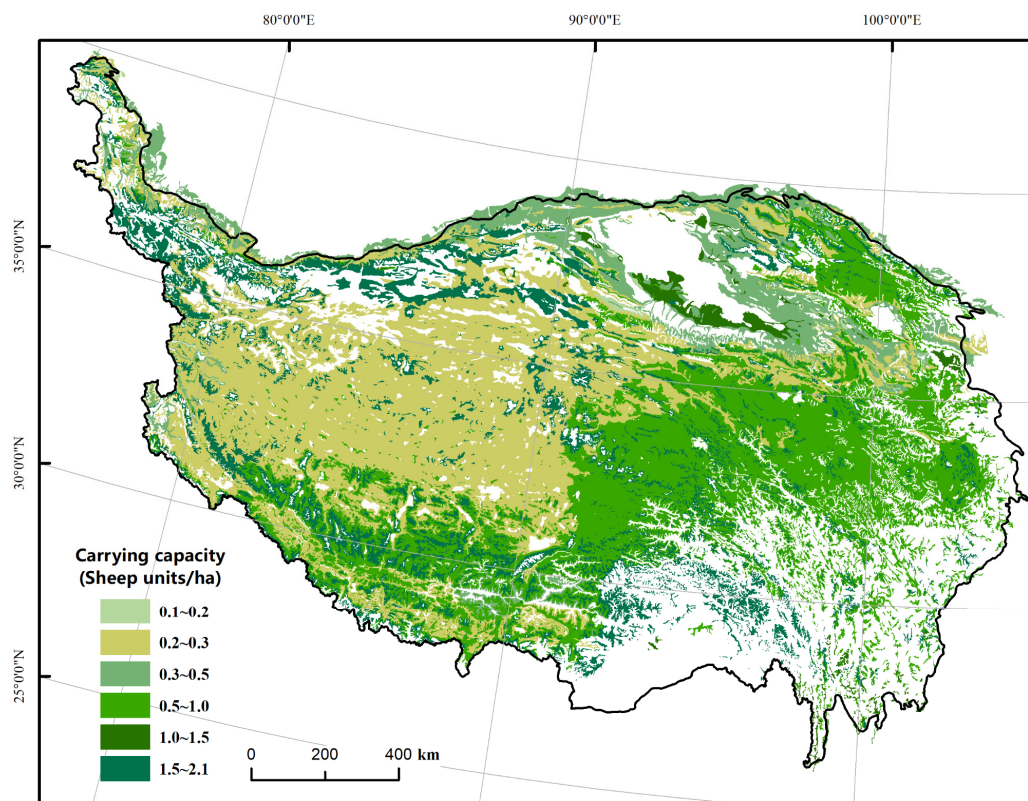


Fig. A2 Spatial distribution of livestock exposure estimated from vegetation distribution

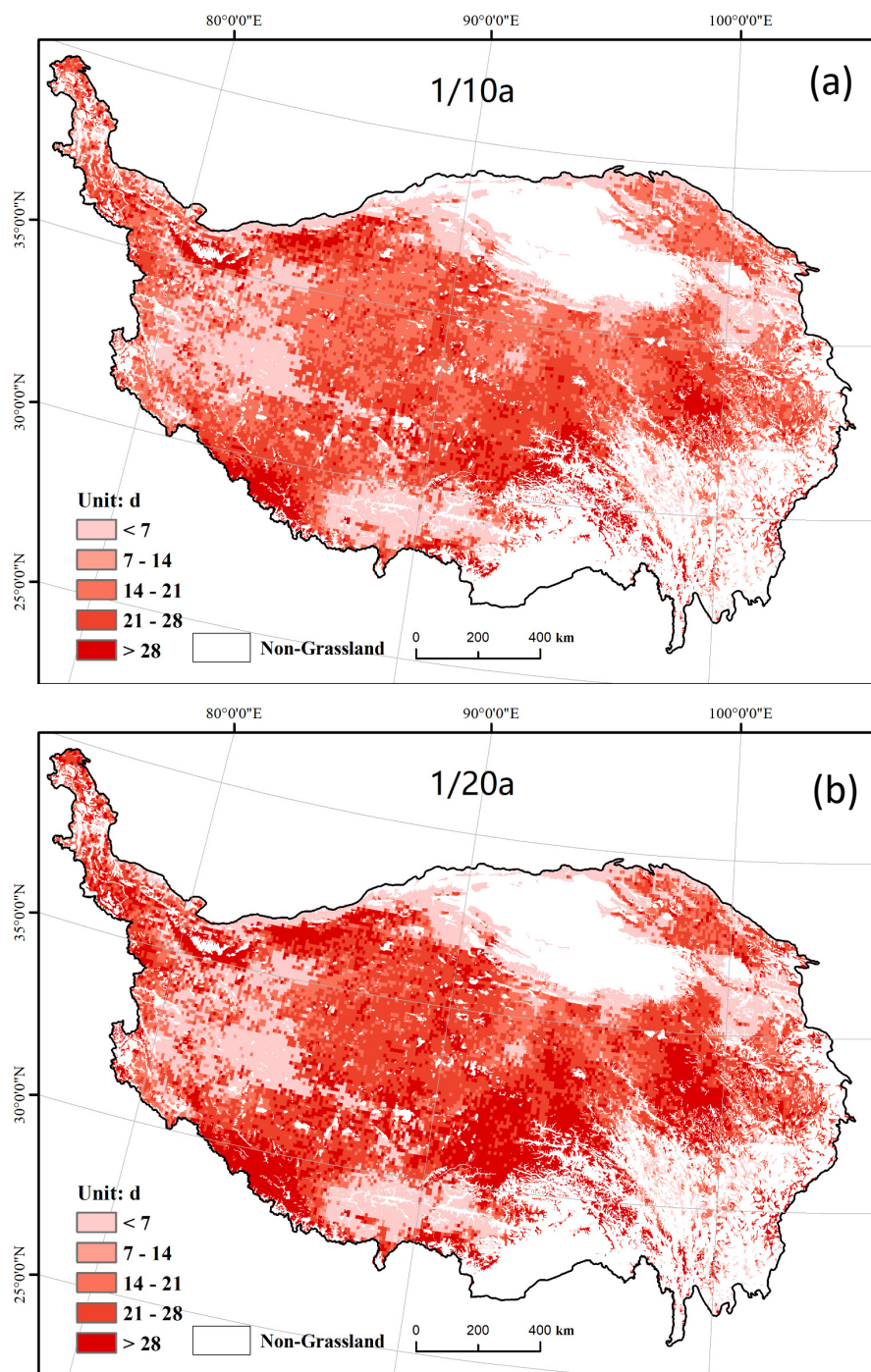


Fig. A3 Gridded duration of a single disaster event by return period: (a) 1/10a; (b) 1/20a



Table A1 Look-up table of carrying capacity by grassland type in the QTP

Grassland type	Fresh grass yield (kg/ha)	Annual grazing rate (%)	Grassland required per sheep unit (ha/unit)	Carrying capacity (sheep unit/ha)
Alpine meadow	1452	50	305.70	0.74
Alpine steppe	677	40	819.30	0.27
Alpine meadow-steppe	689	45	745.20	0.30
Alpine desert-steppe	554	35	1077.30	0.21
Alpine desert	519	30	988.95	0.23
Temperate steppe	3018	40	170.10	1.32
Temperate desert	683	30	1183.50	0.19
Temperate desert-steppe	611	35	840.75	0.27
Lowland meadow	3498	50	127.50	1.76
Mountain meadow	3879	55	132.30	1.70

Note: Figures were adapted from (Xin et al., 2011) and (Land Management Administration of Tibet Autonomous Region, 1994)